Published by :
http://www.ijert.org

International Journal of Engineering Research & Technology (IJERT)
ISSN: 2278-0181
Vol. 6 Issue 01, January-2017

Computational Analysis on Gas Flame Acceleration and Detonation using Propane-Air Mixture

[1]Arunkumar.K
[1]Asst Professor,
Department of Aeronautical Engineering,
KCG College of Technology
Chennai, Tamil Nadu.

[2]Vijaya Prakash. R
[2]Asst Professor,
Department of Aeronautical Engineering,
KCG College of Technology
Chennai, Tamil Nadu.

[3]Adhil Sharief
[3]Asst Professor,
Department of Aeronautical Engineering,
KCG College of Technology
Chennai, Tamil Nadu.

[4]Jagadeesh. R
[4]Student,
Department of Aeronautical Engineering,
KCG College of Technology
Chennai, Tamil Nadu.

***Abstract*:- The computational analysis is to understand the mechanism of flame acceleration, propagation and deflagration-to detonation transition process. The deflagration to detonation transition is the process between subsonic wave to supersonic wave propagation. In this study, 2dimensonal axis symmetric tube is considered and the stoichiometric mixture of propane-air mixture gaseous fuel is used with pressure based solver with absolute velocity formulation for this computational analysis using ANSYS-Fluent Computational Fluent Dynamics software package. The deflagration-to detonation process was captured for given time step and from this, an idea about the mechanism involved in deflagration-to detonation process is obtained. From a result the temperature, pressure, velocity, density and sound speed plot, it is clear that there will be sudden change at detonation wave propagation point. From the species mass fraction , net mass reaction rate and properties plots t is also observed that the chemical reactions changes takes place during the process of detonation.**

I. INTRODUCTON

A. DEFLAGRATION

The process initiates to accelerate the flame, when the propane-air mixture is allowed to burn. Deflagration is subsonic wave.

B. DETONATION

The shock wave travelling through the combustible mixture compresses and heats the gas behind the shock front. If the shock wave is sufficiently strong, then the rise in temperature may be sufficient to ignite combustion behind the shock front. It is the final stage of process. Detonation is supersonic wave propagates from subsonic wave

C.RANKINE-HUGONOIT CURVE

The solution of any steady state deflagration and detonation waves lie on the Hugonoit curve, which can be divided into several branches and regimes, corresponding to different types of combustion waves.

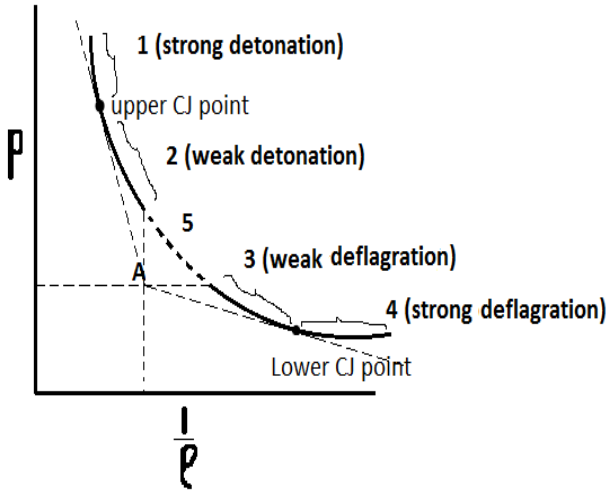

Fig 1.Rankine-Hugonoit curve

In the figure 1 shows the region q is strong detonation, the gas velocity relative to the wave front is slowed down substantially from supersonic speed to subsonic.

The region 2 is weak detonation, the gas velocity relative to the wave front is slowed down substantially from supersonic speed to subsonic, but the burned mixture still has a velocity greater than that of speed.

The region 3 is weal deflagration; gas velocity relative to the wave front is accelerated from a subsonic velocity to a higher subsonic velocity.

International Journal of Engineering Research & Technology (IJERT)
ISSN: 2278-0181
Vol. 6 Issue 01, January-2017

The region 4 is strong deflagration; gas velocity relative to the wave front is accelerated substantially from subsonic to supersonic.

The point A1 which is usually called the origin of the Hugonoit plot. From the graph: the curve is thus divided into five regions the two tangent points to the curve are called velocity point upper and lower. Regions of possible solutions are constructed by drawing tangents to the curve through the point A, and vertical and horizontal lines from A. In the 5th region, the Rayleigh line expression implied that u1 is imaginary. The 5th region is shown to be a physically impossible region. From the symbol p and ρ indicates pressure and density.

C. DEFLAGRATION TO DETONATION TRANSITION

DDT is the process starts from the mild ignition the flame propagates as laminar speed and becomes laminar flame due to the hydrodynamic and diffusion instabilities the flame gets wrinkle flame and the process of increase of turbulence intensity and decrease of length scale flame becomes turbulent flame and next to this process there will be a shock initiation that region is called deflagration –to- detonation transition. In this region detonation will occur. During the process of deflagration –to- detonation transition, deflagration becomes detonation and a usual slow flame accelerates spontaneously with velocity increased by 3 orders of magnitude until an explosion occurs and develops into a self-sustained detonation.

II. CFD MODELLING OF DETONATION AND METHODOLOGY

A. CFD MODELLING OF DETONATION AND METHODOLOGY

In Computational Fluid Dynamics, Fluent is used for this computational works along with the CHEMKIN reaction design software is used to solve chemical equations. For this study propane-air mixture gaseous fuel is used for the computational analysis of detonation process.

PROBLEM DEFINITION

The schematic diagram of the computational domain and the computational mesh used for this study are shown in Figs 1 and 2. A 2D axisymmetric tube introduces the stoichiometric propane-air mixture equivalence ratio, Φ=1 at an inlet temperature of 298K. The ensuing combustion involves several complex reactions between C3H8, CO2, CO, H2O, NO, O2, O, H, N, OH, N2, and H2. The steps used to model this problem are described below. The results are also discussed below.

B. COMPUTATIONAL DOMAIN AND MESH

The 2D axisymmetric tube with length 1m and height 20 mm is used for the computational works. This detonation tube introduces the stoichiometric mixture of propane-air at an initial temperature of 298K and atmospheric pressure of 101325Pa. the mesh size is 20000 cells is found adequate for this problem because two important criteria takes place in this computational works are gradient adaption and partitioning. The computational domain and computational mesh is shown in figure 1.

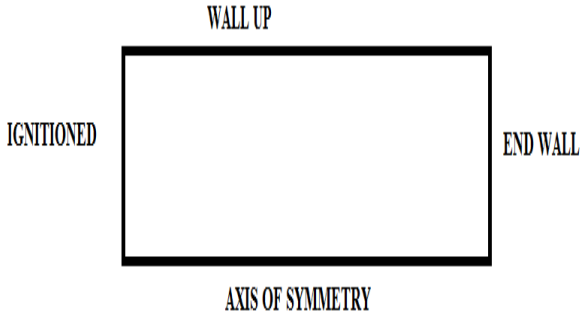

Fig 1. Computational domain

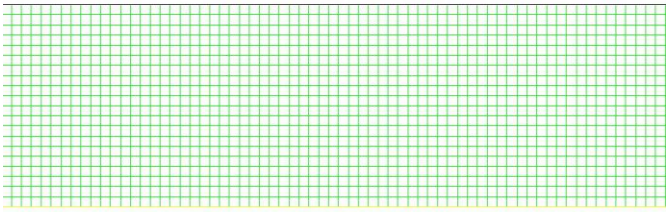

Fig 2.Computational mesh

It was appropriate to use a 2D axisymmetric model for these computational studies. The tube with one end open and other end is closed is shown above figure and normal mesh without adaption is shown in above figure. Mesh quality is orthogonally ranges from 0 to 1, where values close to 0 correspond to low quality. Minimum orthogonal quality is 8.94397e-01 a maximum aspect ratio is 1.41443e+00.

C. .ADAPTIVE GRIDDING

Adapts the mesh based on the gradients of the selected scalar quality, in this study adaptive gridding is based on the temperature gradient. This option is used because for the defined point, the mesh automatically adapts itself where the better solution is required. Adaptive gradient is used to get detailed solution about chemical reactions and limiting the time.

International Journal of Engineering Research & Technology (IJERT)
ISSN: 2278-0181
Vol. 6 Issue 01, January-2017

X min (m) = 0.00674395; x max (m) = 0.01004813
Y min (m) = 0.00089129; y max (m) = 0.00014745

For the above defined point in the domain, the mesh automatically adapts based on the temperature gradient. The adapted mesh is shown below Figure 3.

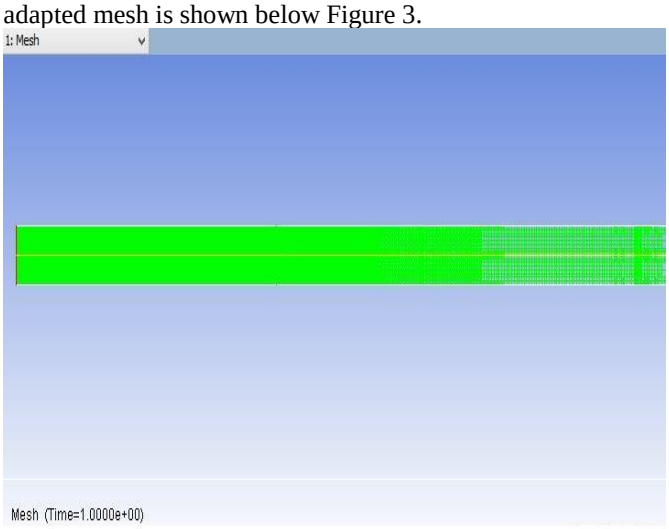

Fig 3.Adaptive gridding based on temperature gradient mesh.

The defined point is very close to the inlet so the mesh was finely adapted near the inlet and it is shown in the above figure. Partitioning is another important criteria in this computational works. Choosing a point near to inlet so that it is the ignition point in this computational work.

D. PARTITIONING

In this study principal axes method is used for partitioning,

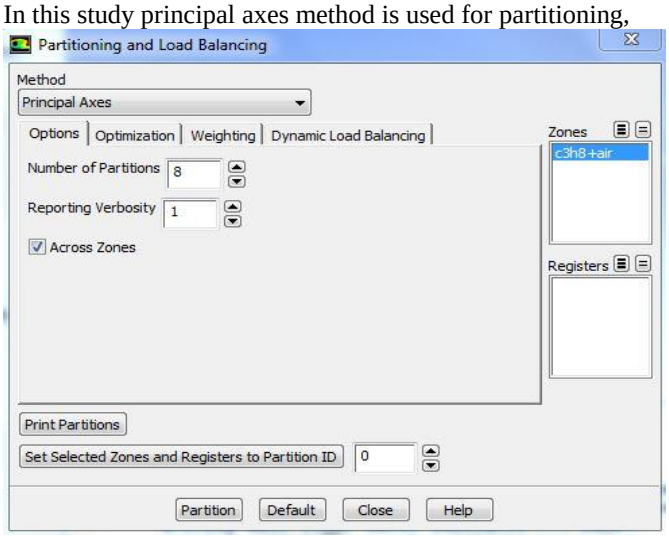

Fig 4.Portioning and load balancing setup.

The figure 4 is partitioning setup shows the partitioning method and partition count. Dividing the domain into 8 partitions using principal axes. The partition statistics table is shown below figure 5

```
>> Dividing domain into 8 partitions using Principal Axes.
..... 7 bisections.
   Time = 0.156001 seconds.
   Done.

>> 8 Partitions:
   ---------------------------------------------------------------------
   Collective Partition Statistics:      Minimum   Maximum   Total
   ---------------------------------------------------------------------
   Cell count                            4114      9216      67970
   Mean cell count deviation             -51.6%    8.5%
   Partition boundary cell count         23        159       1000
   Partition boundary cell count ratio   0.6%      1.7%      1.5%

   Face count                            9450      18656     138490
   Mean face count deviation             -45.6%    7.4%
   Partition boundary face count         24        160       504
   Partition boundary face count ratio   0.3%      0.9%      0.4%

   Cell weights                          2e+04     6e+04     4e+05
   Mean cell weight deviation            -51.6%    8.5%

   Partition neighbor count              1         2
   ---------------------------------------------------------------------
   Partition Method                      Principal Axes
   Stored Partition Count                8
Done.
```

Fig 5.Partition statistics

E. SOLUTION SETUP

The below figure 6 is the solution setup for this computational works, pressure-based solver, absolute velocity formulation, transient case, axisymmetric, double precision is used.

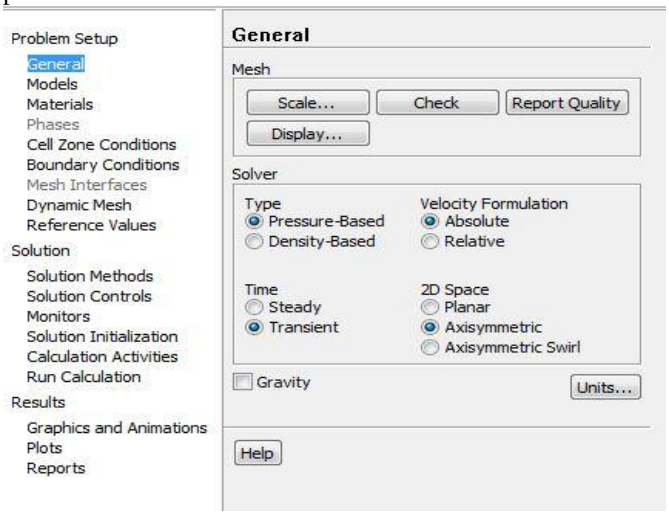

Fig 6.Fluent solution setup

F. MODELS

The table 1 is model setup option in fluent, time is unsteady with 1st order implicit method, energy and species transport are enabled, viscous is laminar, theory of species transport and finite-rate chemistry is described below.

s.no	Model	Settings
1	Space	Axisymmetric
2	Time	Unsteady, 1st-order implicit
3	Energy	Enabled
4	Viscous	Laminar
5	Species transport	Enabled

Table 1.Model setup

International Journal of Engineering Research & Technology (IJERT)
ISSN: 2278-0181
Vol. 6 Issue 01, January-2017

G. THEORY OF SPECIES TRANSPORT AND FINITE-

The species model setup for setting parameters for species transport is shown in figure 7.

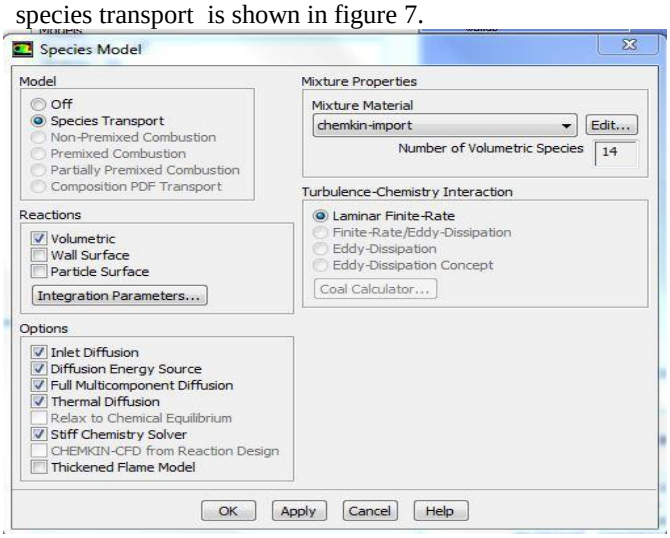

Fig 7 Species model setup for setting parameters for species transport

H.MATERIALS

The materials setup allows the properties for any fluid or solid materials in ANSYS fluent simulation. In this present study materials as propane air mixture is imported from CHEMKIN reaction DESING software. The material selection setup is shown in figure 8.

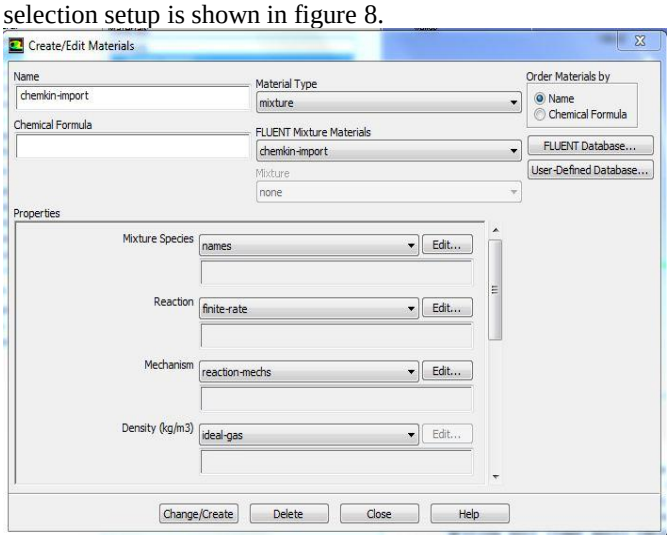

Fig 8. Material selection setup.

I.CELL ZONE CONDITIONS

In this present study fluid type cell zone is used. A fluid zone is a group of cells for which all active equations are solved. The cell conditions are shown in the table 2.

S.NO	CONDITION	VALUE
1	Material name	C_3H_8+Air
2	Source terms	Mass, X-momentum, Y-momentum, species, energy
3	Fixed values	X-velocity, Y-velocity, species, temperature
4	Solid material name	Aluminium

Table 2.Cell condition setup

J.BOUNDARY CONDITIONS OUTLET BOUNDARY CONDITIONS

The boundary conditions at the outlet plane were specified as follows: Pressure, Pa=101325N/m^2 and species mass fraction, C_3H_8= 0.034, O_2= 0.225 for the velocity coupling, coupled scheme was employed. The boundary conditions for outlet are shown in the table 3.

s.no	Condition	Value
1	Gauge pressure (Pascal)	0
2	Back flow temperature (K)	300
3	Axial-component of flow direction	1
4	Radial-component of flow direction	0
5	X-Component of axis direction	1
6	Y-Component of axis direction	0
7	Upper limit of absolute pressure (Pascal)	5000000
8	Lower limit of absolute pressure (Pascal)	1

Table 3.Boundary condition setup for outlet

K.WALL BOUNDARY CONDITIONS

The thermal boundary condition was set at a fixed heat flux of zero, while the walls were set as not moving. The no slip conditions were prescribed for wall shear stress. The boundary condition for wall is shown in the table 3.

L.SOLUTION METHODS

The solution methods setup allows to specify various parameters associated with solution method to be used in the calculation. In the pressure velocity coupling, SIMPLEC algorithm scheme is used among five types of scheme SIMPLE, SIMPLER, PISO and COUPLED.

s.no	Variable	Relaxation factor	Discretization scheme
1	Pressure	0.4	Second order
2	Density	1	Second order upwind
3	Momentum	0.8	Second order upwind
4	Species	1	Second order upwind
5	Energy	1	THIRD-ORDER MUSCL

Table 5.Discretization scheme and relaxation factor for different variables

In the present study the initial spark was supplied by patching a high temperature field into a region of the model that contained a sufficient premixed fuel, air, product mixture for ignition to occur.

This process is the initiation of detonation to occur.

III. .RESULTS AND DISCUSSIONS

A. *IDDT CONDITION CONTOUR*

The process of deflagration to detonation transition is shown in two ways in figure 1 and figure 2. The figure shows the deflagration detonation transition condition and also shows process involves after detonation. The figure 2 shows clear vision of the detonation wave propagation. During the process of deflagration detonation transition a usual slow flame accelerates spontaneously with velocity

International Journal of Engineering Research & Technology (IJERT)
ISSN: 2278-0181
Vol. 6 Issue 01, January-2017

increased by 3 orders of magnitude until an explosion occurs develops in to a self-sustained detonation.

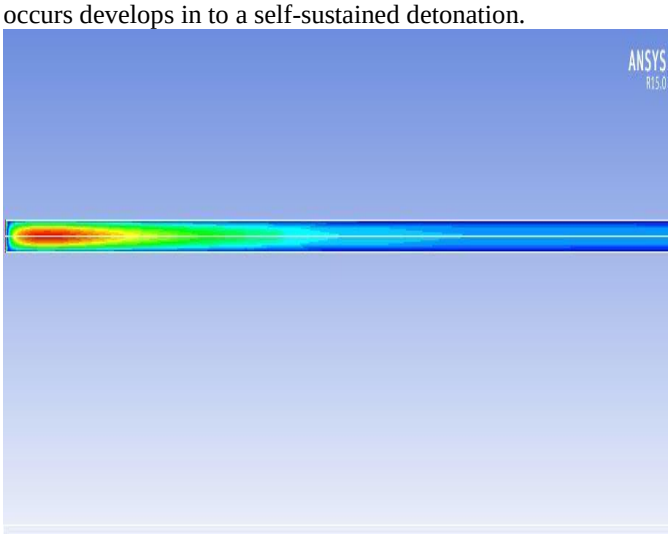

Fig 1.Deflagration detonation transition condition contour

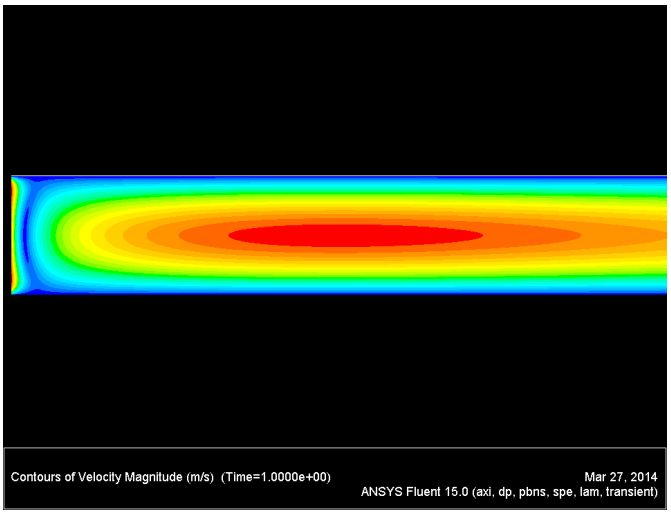

Fig 2.Clear vision of detonation wave propagation contour

B. *PROCESS OF DETONATION WAVE PROPAGATION*

The overall length of the tube is 1 m and from the ignition point flame initiate and flame propagates as laminar flame and becomes wrinkle flame due to hydrodynamic and diffusion instabilities, flame accelerates and becomes deflagration wave. This deflagration wave transition to detonation wave is at 0.04m. Each and every process takes place before detonation is shown in figure 4.3.

Deflagration wave propagation speed M=V/a

Velocity V=340 m/s and sound speed a= 960m/s M=0.35

Detonation wave propagation speed M=V/a

Velocity V=1700 m/s and sound speed a=960 m/s m=1.77

Detonation wave propagates at subsonic speed 0.35 and detonation wave propagates at supersonic speed 1.77. The velocity, temperature, pressure, density, sound speed, species mass fraction and properties are shown in the graph for detailed understanding of detonation process.

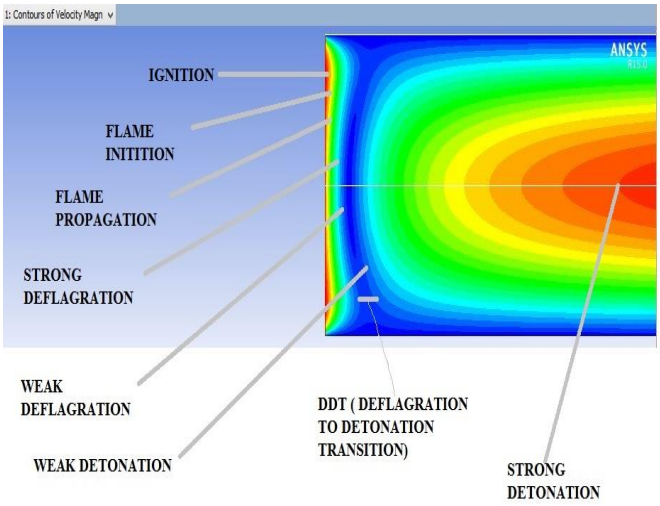

Fig 3.Process of detonation

The flame initiation, flame propagation, deflagration, deflagration to detonation transition process is shown in the figure 3. The detonation wave initiates at 0. 04m in 1m tube and deflagration detonation transition takes place at 0.02 to 0.04m in 0.15 seconds. The velocity, temperature, pressure, density, sound speed, species mass fraction and properties are shown n the graph for the clear understanding of detonation process.

C. *PRESSURE, VELOCITY, TEMPERATURE AND SOUND PLOT*

The pressure, velocity, temperature and sound speed plot helps to understand the detonation process detail. The species mass fraction, net reaction rate and properties plot helps to understand the chemical reaction takes place in the detonation process.

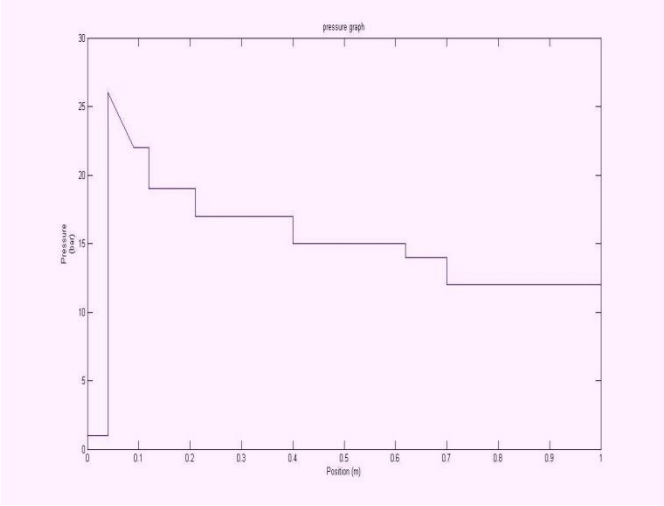

Fig 4.Pressure plot along the axis

From the figure 4, it is observed that the detonation process takes place at 0.04m n 1m tube, the pressure suddenly increased at this region and step by step slowly gets decreased. Therefore the pressure at this increased point is detonation pressure is 25bar.

International Journal of Engineering Research & Technology (IJERT)
ISSN: 2278-0181
Vol. 6 Issue 01, January-2017

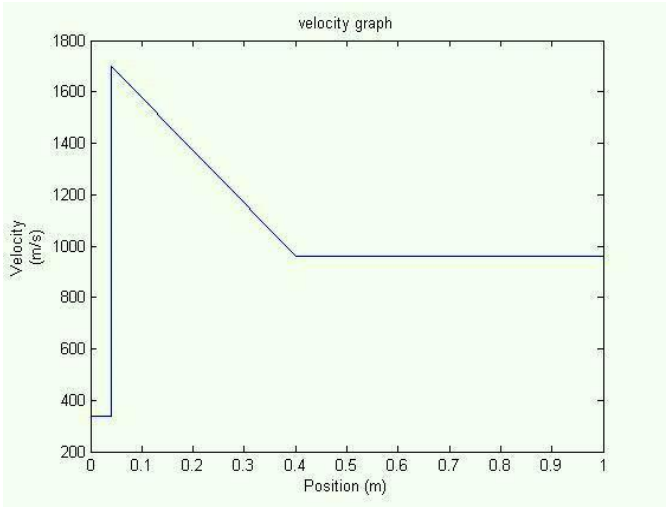

Fig 5.Velocity plot along the axis

From the figure 5, it is observed that velocities gets suddenly increased at a region 0.04m and decreased at a region 0.4m after that maintaining the constant level till at the end of the tube therefore from the result graph detonation velocity s 1700 m/s.

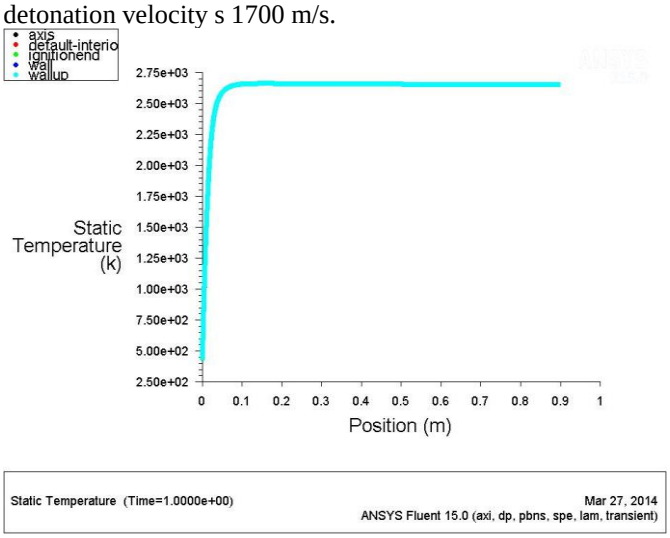

Fig 6.Temperature plot along the axis

From this above figure 6 t is observed that the temperature gets increased at 0.04m and after this increment the temperature maintain a constant level. Therefore, increased high temperature is detonation temperature that the value is 2600k.

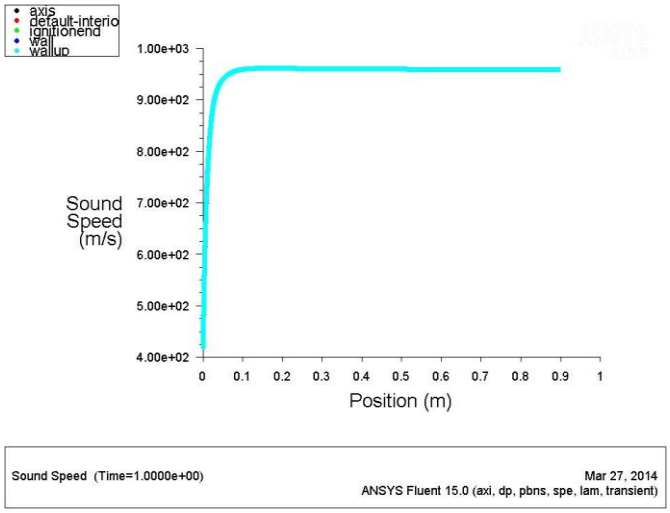

Fig 7.Sound speed plot along the axis

From the given figure 7 it is observed that the sound speed gets increased at 0.04m with a speed of 960m/s. the detonation velocity must be greater that sound speed. The statement is true by observing sound speed plot and detonation velocity plot. The detonation velocity s 1700m/s and sound speed is 960m/s, therefore detonation velocity is greater than sound speed.

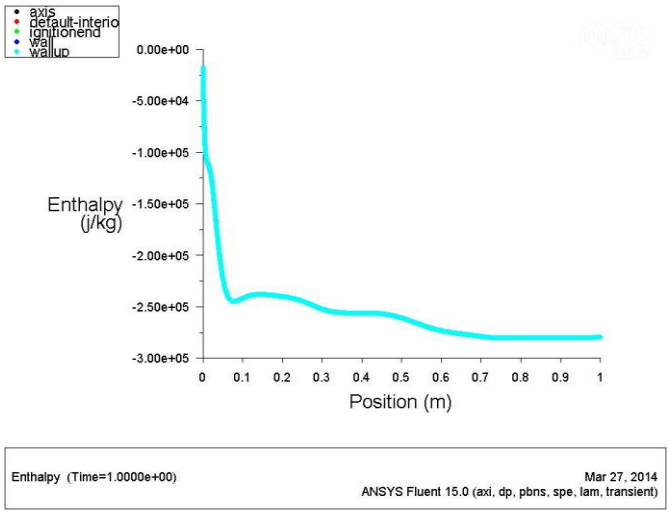

Fig 8.Enthalpy plot along the axis

From the figure 8 it is observed that the enthalpy gets suddenly decreased at detonation initiation point 0.04m and after detonation it is slowly gets decrease at 0.7m and after this maintaining constant level.

International Journal of Engineering Research & Technology (IJERT)
ISSN: 2278-0181
Vol. 6 Issue 01, January-2017

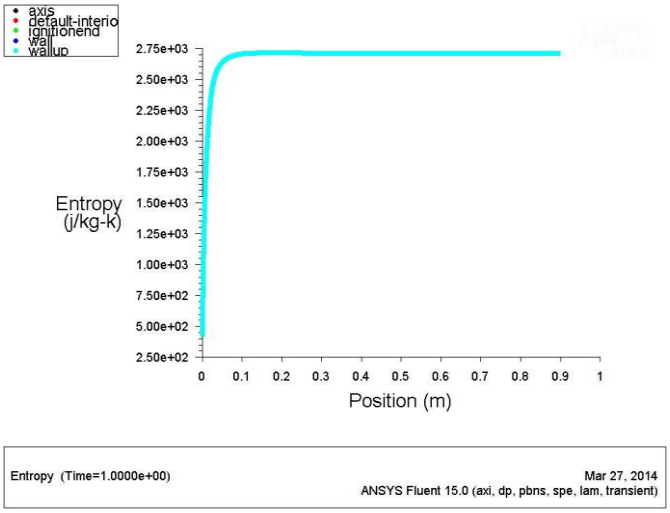

Fig 9.Entropy plot along the axis

From the figure 9 it is observed that the enthalpy gets suddenly decreased at detonation initiation point 0.04m and after detonation slowly gets decrease at 0.7m and after this maintaining constant level.

REFERENCE

[1] K. He, I. P. Androulakis, and M. G. Ierapetritou, "Multi-element flux analysis for the incorporation of detailed kinetic mechanisms in reactive simulations," Energy and Fuels, vol. 24, pp. 309-317, 2010.

[2] N. Peters and F. A. Williams, "The asymptotic structure of stoichiometric methaneair flames," Combustion and Flame, vol. 68, pp. 185-207, 1987.

[3] U. Maas and S. B. Pope, "Simplifying chemical kinetics: Intrinsic low-dimensional manifolds in composition space," Combustion and Flame, vol. 88, pp. 239-264, 1992.

[4] S. H. Lam and D. A. Goussis, "CSP method for simplifying kinetics," International Journal of Chemical Kinetics, vol. 26, pp. 461-486, 1994.

[5] L. Petzold and W. Zhu, "Model reduction for chemical kinetics: An optimization approach," AIChE Journal, vol. 45, pp. 869-886, 1999.

[6] K. Edwards and T. F. Edgar, "Reaction set simplification using variable selection techniques," Chemical Engineering Science, vol. 55, pp. 551-572, 2000.

[7] I. P. Androulakis, "Kinetic mechanism reduction based on an integer programming approach," AIChE Journal, vol. 46, pp. 361-371, 2000.

[8] O. Herbinet, W. J. Pitz, and C. K. Westbrook, "Detailed chemical kinetic mechanism for the oxidation of biodiesel fuels blend surrogate," Combustion and Flame, vol. 157, pp. 893-908, 2010.

[9] Y. Shi, H. W. Ge, J. L. Brakora, and R. D. Reitz, "Automatic chemistry mechanism reduction of hydrocarbon fuels for HCCI engines based on DRGEP and PCA methods with error control," Energy and Fuels, vol. 24, pp. 1646-1654, 2010.

[10] T. Lu and C. K. Law, "A directed relation graph method for mechanism reduction," 2005, pp. 1333-1341.